

Chemical factors controlling the steady-state distribution of mixed carbonate-siliciclastic sediments in Bayona Bay (northwest Spain)

*S. Fernández-Bastero*¹, *I. Alejo*¹, *M. A. Nombela*¹, *S. García-Gil*¹, *G. Francés*¹,
*B. Rubio*¹, *M. Pérez-Arlucea*¹, *R. Jiménez*², *D. Rey*², *A. Bernabeu*², *O. Pazos*¹,
*L. Gago Duport*¹, *F. Vilas*¹ and *A. Santos*³

¹ Departamento de Geociencias Marinas. Facultad de Ciencias. Universidad de Vigo. Apdo. 874. 36200 Vigo (Pontevedra), Spain

² Departamento de Estratigrafía. Facultad de Ciencias Geológicas. Universidad Complutense de Madrid. Avda. Complutense, s/n. Madrid. Spain

³ Departamento de Cristalografía-Mineralogía. Facultad de Ciencias del Mar. Universidad de Cádiz. Apdo. 40 Cádiz, Spain

Received October 1997. Accepted April 1998.

ABSTRACT

The relative space distributions of single mineral constituents in mixed terrigenous-carbonated sediments of the Bayona Bay have been analysed. In order to determine the existence of different mixing mechanisms, a study comparing the general sedimentary trends resulting from the average patterns and the single mineral behaviour, reflected in the single-mineral mapping, was carried out.

The relative abundance of all mineral phases in surface sediment samples was first determined by quantitative X-ray powder diffraction data, using the Rietveld method. This procedure enabled us to create specific maps for both the minerals forming the terrigenous fraction and the different calcium carbonate polymorphs involved in the carbonatic component.

A cross-linked behaviour between the carbonate facies and the terrigenous minerals involved in the calcium carbonate generation was found, suggesting the existence of a chemical control mechanism which, through dissolution-crystallization processes, constrains the mixed environment's long-term evolution.

In the general framework of the region studied, these relations operate for the relative amount of plagioclase to calcium carbonate. The existence of dissolution and growth between both minerals, favoured by the high rate of removal, is proposed, yielding a final crossed pattern, representative of the steady-state. Furthermore, a specific analysis, restricted to the region of low rate of material removal and maximum amount of intermixed sediments, clearly shows an anisotropic distribution for every calcium carbonate polymorph (calcite and aragonite). These correlate with the biotite distribution, and can be connected to local variations in seawater Mg/Ca ratio, induced by biotite weathering.

Key words: Carbonate-siliciclastic sediments, dissolution-crystallisation, mineral growth processes, shallow waters, sedimentary dynamic.

RESUMEN

Mecanismos de control sobre la distribución estacionaria en sedimentos carbonatados-siliciclásticos en la bahía de Bayona (noroeste de España)

En este trabajo se analiza de forma específica la distribución espacial de cada uno de los minerales involucrados en sedimentos mixtos terrígenos-carbonatados de la bahía de Bayona y se compara con la distribu-

ción global de sedimentos, tal como resulta de análisis granulométricos, con el fin de determinar la existencia de diferentes mecanismos de mezcla entre los minerales de ambas fracciones.

El contenido porcentual en peso de cada fase mineral, en muestras superficiales de sedimento, se determinó a partir de datos cuantitativos de DRX, empleando el método de Rietveld. Este procedimiento nos ha permitido realizar mapas específicos de distribución, tanto para cada mineral de la fracción terrígena como para cada uno de los diferentes polimorfos de carbonato cálcico en la componente carbonatada.

Como resultado de este estudio comparativo, se ha encontrado una correlación, en la distribución espacial y granulométrica, de las facies carbonatadas y los minerales terrígenos implicados en la generación de carbonato cálcico. Un posterior análisis de este resultado sugiere la presencia de mecanismos químicos de control que regulan la interacción entre siliciclastos y carbonatos mediante procesos de disolución-cristalización mediados por el agua del mar.

El estudio se ha realizado a dos escalas. En el ámbito general de la bahía de Bayona, las relaciones de distribución observadas entre plagioclasas y carbonato cálcico pueden ser explicadas, dentro del balance global del Ca^{2+} disuelto en el agua del mar, mediante la meteorización química de las plagioclasas y la consiguiente generación de carbonatos. En este caso, los patrones de distribución reflejan la aproximación a un estado estacionario mediante sucesivos eventos de mezcla asociados a la alta removilización material en el medio, tanto para la distribución porcentual en peso como para la distribución granulométrica entre ambos minerales. Finalmente, se realiza un análisis particularizado en una región con baja tasa de removilización y donde la interacción entre sedimentos de ambas fracciones es máxima. El resultado muestra claramente una distribución espacial anisótropa para cada uno de las fases de carbonato cálcico (calcita y aragonito). La abundancia relativa de cada uno de los polimorfos, así como el contenido en Mg^{2+} de la calcita, ha sido correlacionado con la distribución de la biotita y explicado a partir de las diferencias de solubilidad en función de la alta relación $\text{Mg}^{2+}/\text{Ca}^{2+}$ en el agua de mar que resulta, localmente, de la meteorización química de dicho mineral.

Palabras clave: Sedimentos terrígenos-carbonatados, disolución-cristalización, crecimiento de minerales, aguas someras, dinámica sedimentaria.

INTRODUCTION

The general sedimentation trends in mixed siliciclastic-carbonated environments are usually related to dynamic processes, considered the main factors commonly influencing both the siliciclastic and carbonated fractions, and given an average space-distribution marked by grain-size factors. However, the mixing of terrigenous sediments and carbonate materials involves a variety of sedimentological, biological and chemical processes, which are oversimplified in a model exclusively based on grain-size distribution. This is of particular importance when there is evidence of process and product control from the siliciclastic environments to the carbonatic ones.

According to Mount (1984), the following categories of 'mixing' can be considered: 1) 'punctual mixing' during rare sedimentation events of high intensity; 2) *in situ* mixing by the new generation of carbonates within siliciclastic sediments; 3) mixing by the contact between both facies.

The purpose of the present paper is to analyse the existence of specific control mechanisms which, for a particular steady-state distribution of the the siliciclastic fraction (i.e. the averaged sedimentary patterns obtained as results of the above

categorisation of mixing mechanisms 1) and 3)), can induce local variations in the carbonate distribution (i.e. by controlling the *in situ* mixing). These alternate rich-depleted zones can be considered spatial anisotropies, and they act as initial conditions in further general mixing events. Consequently, the time-evolution of the sedimentary pattern can be considered the result of a multi-source system, where the signature of local control mechanisms manifests itself as deviations in the average sedimentary trends, and offers a measure of the relative extents and efficacy of the different mixing mechanisms.

The starting point for this study has been the analysis of the general space-distribution of both terrigenous and siliciclastic fractions resulting from granulometric distributions. In a second step, detailed maps of the specific distribution for each mineral were drawn up. The procedure (see below) was based on quantitative analysis of the XRD patterns of surface sediment samples.

In addition to the study of the general distribution pathways, a detailed analysis of the space-distribution of the different polymorphs of calcium carbonate (calcite and aragonite), together with the relative amount of Mg in calcites indicates a specific behaviour for every polymorph. This study was restricted to

the areas where a maximum mixing between carbonate-terrigenous takes place. A comparative analysis between the relative amounts of carbonate polymorphs to biotite distribution, and further estimates of the Mg released during stoichiometric weathering of biotite, were also performed.

MATERIALS AND METHODS

Sea-floor sediment samples were collected in the Bayona Bay from 29 stations (figure 1), using Van Veen and Shipek grab samplers (Alejo, 1994).

Analysis of the mineral composition of the entire set of samples was performed by X-ray powder diffraction experiments. Step-scan Cu K α XRD data were recorded using a Siemens diffractometer over the 2 θ range 2° to 69.65° at intervals of 0.05° 2 θ and a graphite monochromator. The use of the X-ray

powder diffraction data was focused on obtaining the respective mineral phase fractions (wt %) of both the siliciclastic and carbonate components of the samples. In the latter case, refinements of the calcite cell parameters were used to determine the Mg content.

The carbonatic fraction mainly comprises fragments of bivalves, gasteropods, echinoderms spicules, foraminifera, calcareous algae (*Lithothamnium* sp.) and bryozoans (Alejo, 1994). The main siliciclastic constituents are quartz, K-feldspar, plagioclase, moscovite, and biotite. The average plagioclase composition from the source areas are in the range from Ab₇₀An₃₀ for granitic rocks, and between Ab₇₀An₃₀ to Ab₂₀An₈₀ for metamorphic sources (Rubio-Navas, 1981).

The quantitative analysis of the experimental XRD spectra was performed by using the Rietveld method. Classically, a modal analysis of each mineral component of sedimentary samples can be determined by optical microscope, bulk chemical data and/or X-ray

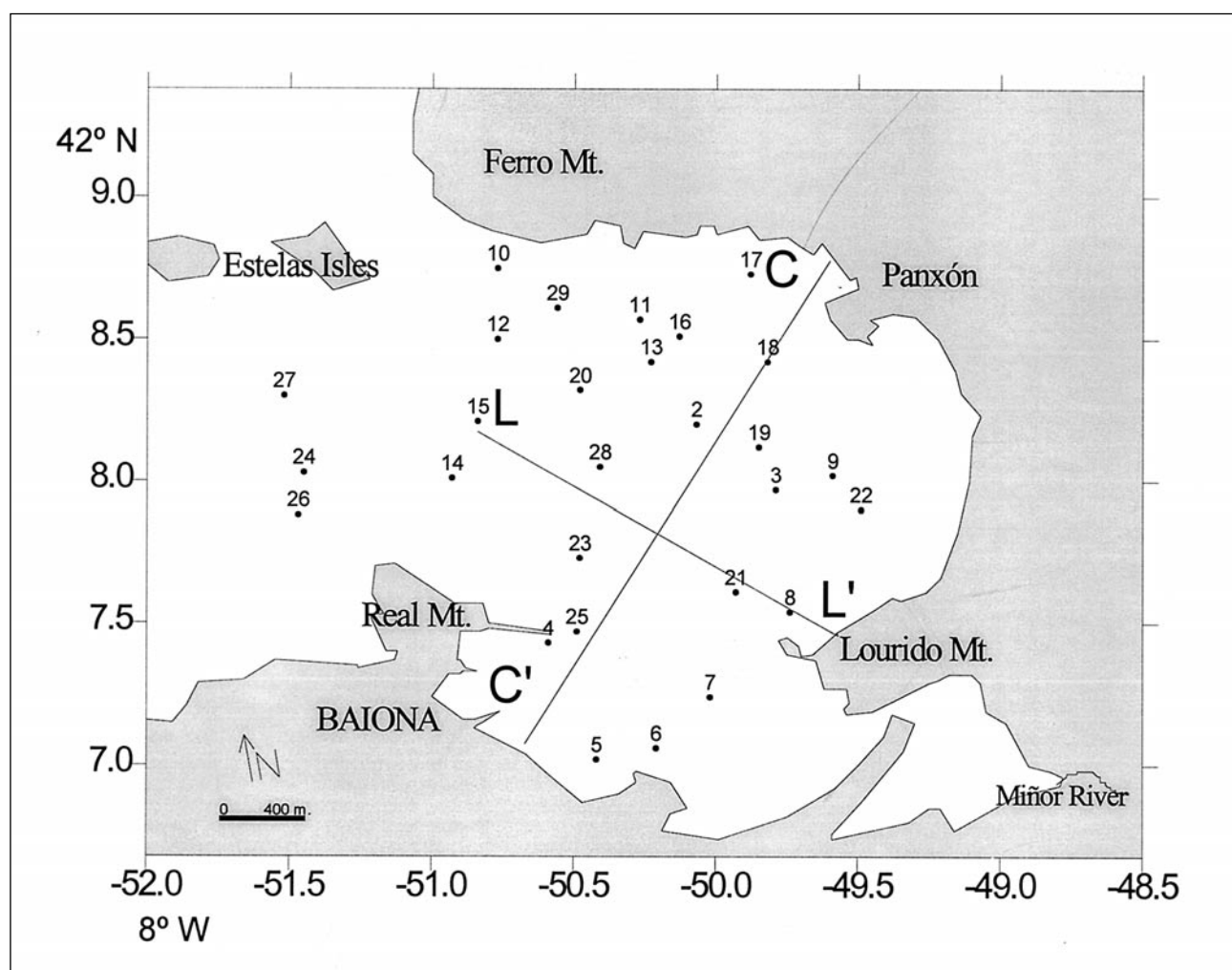


Figure 1. Area under study and sampling locations. The directions LL' and CC' represent the direction of profile lines mentioned in the text

powder diffraction (Mumme *et al.*, 1996). In the past, the analysis method for X-ray powder diffraction data was to fit observed and calculated diffraction patterns using integrated peak intensities (Klug and Alexander, 1974). In recent years, the Rietveld method (Rietveld, 1967, 1969) has become a very powerful tool for quantitative determination of the mineral contents in sedimentary samples, as shown in the recent work of Mumme *et al.* (1996). They have analysed 11 mineral components (e.g. quartz, albite and muscovite) of five sedimentary rocks (arenite, graywacke, slate, mudstone and shale) using this procedure.

In the present paper, the Rietveld refinements of the samples have included the following phases: quartz, calcite, aragonite, kaolinite, biotite, muscovite, microcline and plagioclase. The Fullprof program (Rodríguez, Anne and Pannetier, 1987) was employed in all calculations.

The relative abundances of each phase were determined from the values of scale factors obtained during the refinement (Hill, 1993; Bish and Post, 1993; Post and Bish, 1989). The reliability of the measured wt %, in all the cases, was estimated by the standard deviation values of this parameter.

In addition, the calcite cell parameters were also refined in order to obtain the axial ratio c/a . The Mg contents in the calcite was then determined by using the determinative curves developed by Goldsmith (Goldsmith, Graf and Heard, 1961). In these curves, not only the variations in the cell volume but also the specific distortion induced by different wt % of Mg contents are taken into account and related to the axial ratio c/a . In our case, the following expression has been used:

$$c/a = 3.420 - 0.11X + 0.56X$$

This expression relates the c/a values to the mol fraction (X) of $MgCO_3$ in the carbonate, and has been found to give reliable values for a range of compositions from 0 to 50 mol % of Mg contents (Bischoff, Bishop and McKenzie, 1983). The highest values of Mg contents (on the order of 10 mol %) were in good agreement with the EDX analysis performed on selected samples (Ba-9, Ba-19, Ba-7), shown in figure 1 (Alejo, 1994).

A typical output-plot with the final results from Rietveld analysis is shown in figure 2.

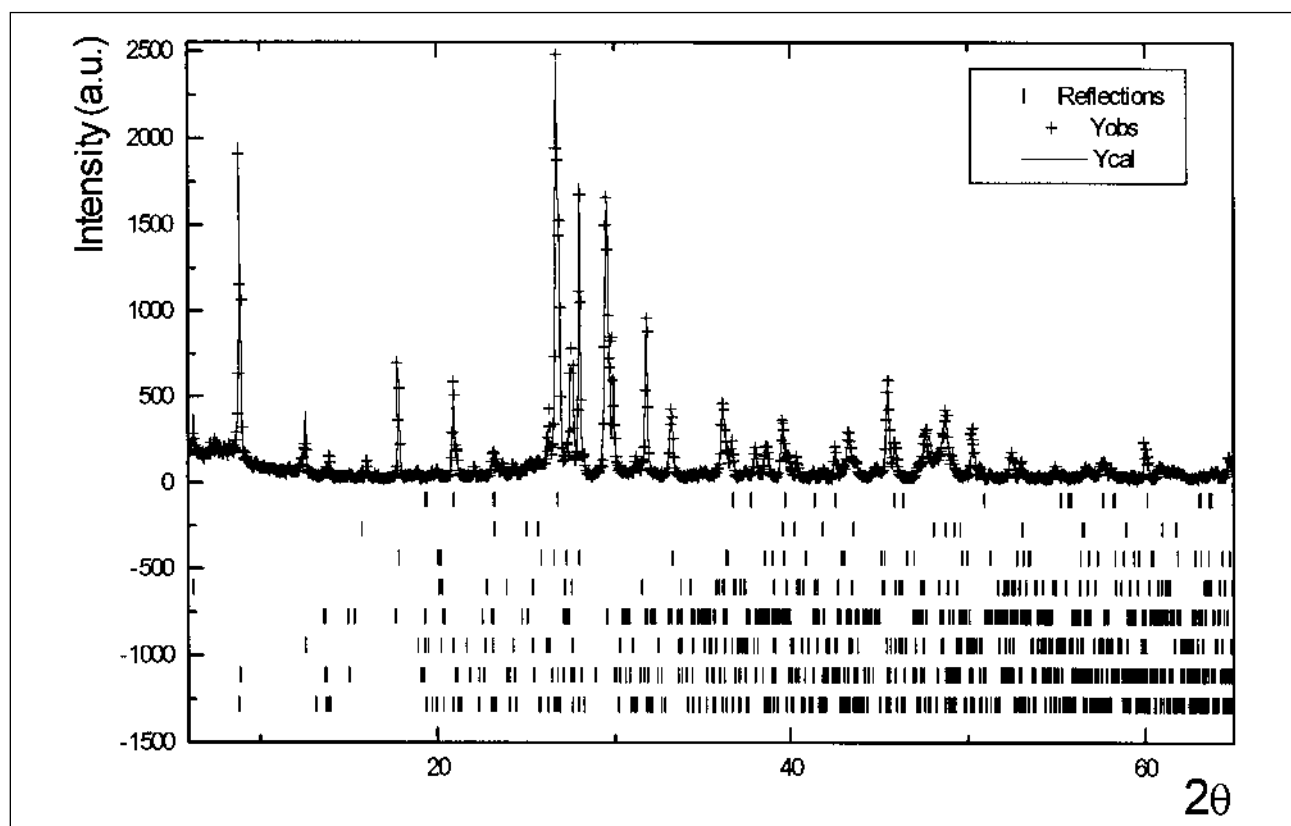


Figure 2. Typical results from the XRD-Rietveld analysis. Crosses represent the experimental diffraction pattern and the continuous line the calculated one. The reflexion marks for the eight minerals involved in the deconvolution are also shown

Finally, specific content maps for each mineral phase, on both siliciclastic and carbonated components, were drawn up in order to compare their spatial distribution with the average distribution obtained by calcimetry and grain-size analysis.

RESULTS AND DISCUSSION

The average sedimentation pattern showing the space distribution of all the terrigenous sediments in Bayona Bay is shown in figure 3. In addition, the grain-size distribution resulting from settling-tube analysis is shown in figure 4.

Comparison between both maps clearly suggests that the grain-size spatial distribution of both fractions is mainly governed by dynamic factors, giving an average pattern that reflects the energy distribution in the environment.

In order to establish specific relationships between carbonate and siliciclastic minerals, deconvolution of the averaged patterns into each single mineral components was performed following the result of the XRD-Rietveld analysis. This was done for quartz, plagioclase microcline, biotite muscovite and kaolinite, the major mineral phases of the terrigenous fraction, as well as for every calcium carbonate polymorph (calcite and aragonite, see figures 5 and 6). The Mg content (mol %) in calcites was also plotted by using the results of the determination based in the axial $(c/a)_{\text{calcite}}$ ratio.

General chemical constraints during siliclastic-carbonate mixing

The 50 wt % contour line, (white line on the contour plots) represents the maximum mixing line

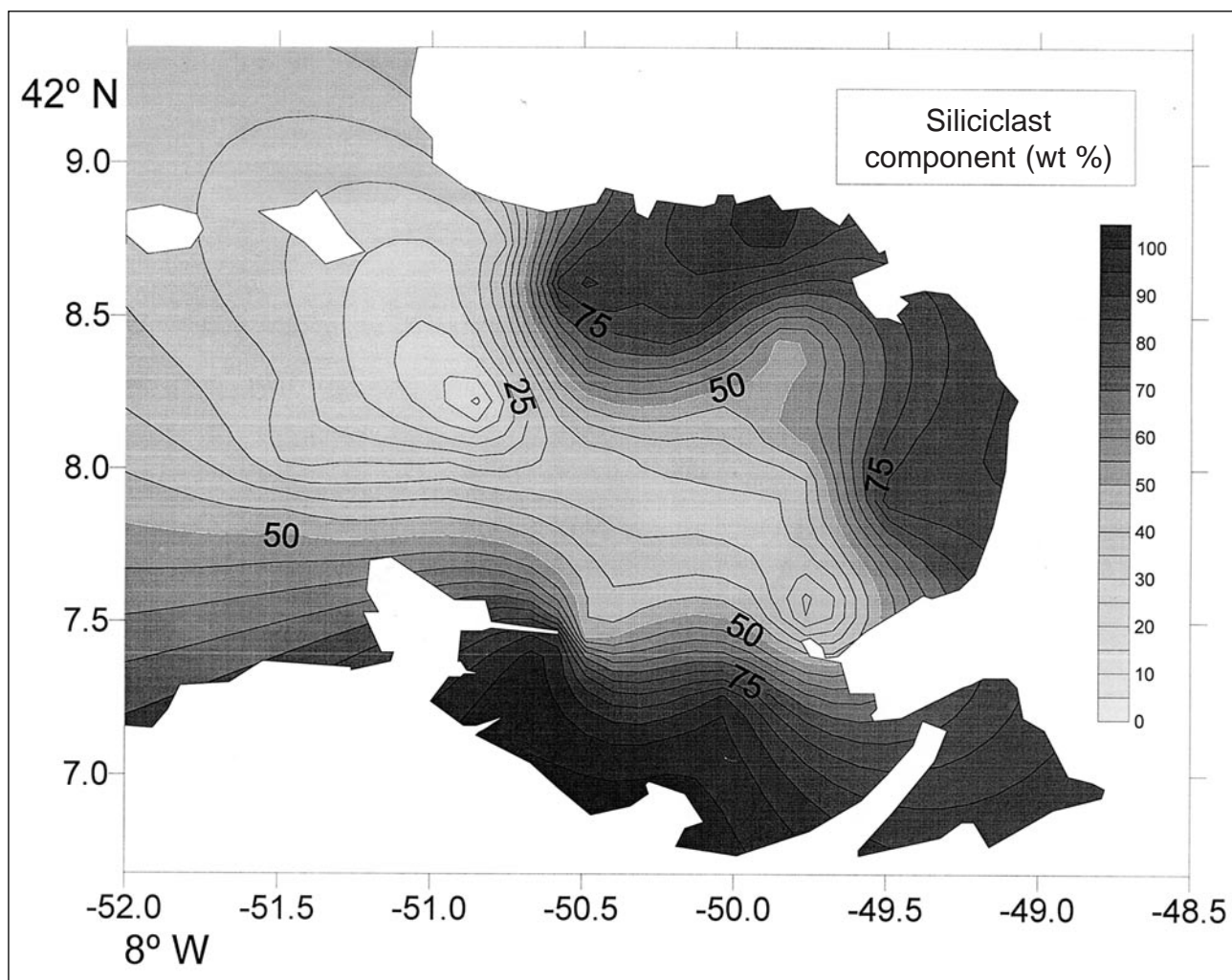


Figure 3. The average sedimentary pattern for the whole siliciclastic fraction (wt %)

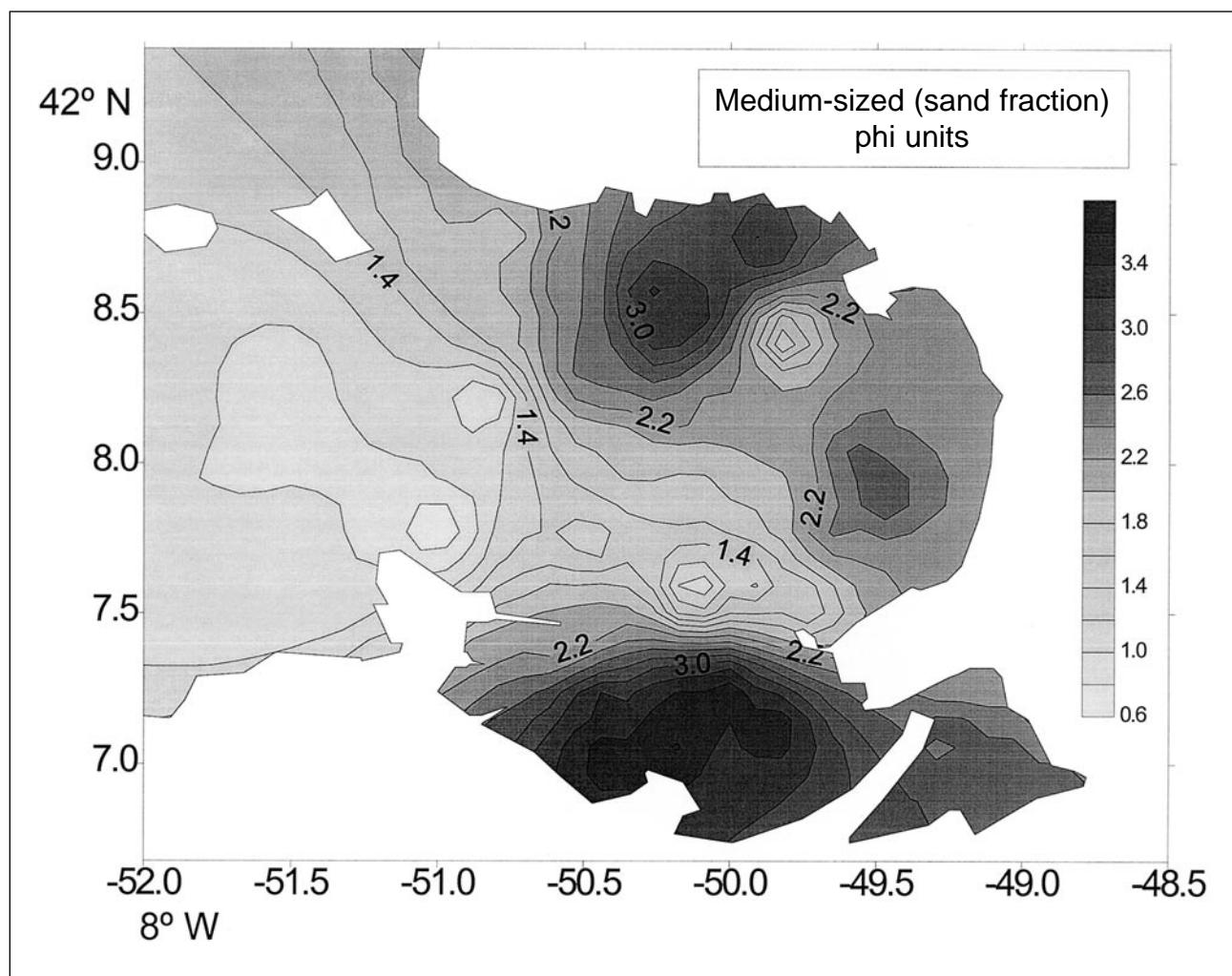


Figure 4. Space-distribution of the average granulometry (phi -scale)

(MML) between both facies. In the following analysis, several results will refer to this line, as it fulfills two requisites: firstly, it is placed in the middle of the region where the siliciclastic-carbonatic interactions can be most effective; secondly, this region fits well with a constant value for the average grain-size (2.6 Phi) as shown in figure 4. Consequently, an anisotropic behaviour in the distribution of each single mineral component through this line reflects the coupling of different processes within the general pathway imposed by the dynamic regime.

In line with this point of view, several specific aspects concerning the space relations between minerals of both fractions are observed. In the terrigenous fraction the most conservative distribution corresponds to the plagioclase minerals. As can be seen in figure 5a, the concentration lines are distributed parallel to the aforesaid MML. This indicates that, at the maximum interchange region,

constant compositional values apply not only for the whole carbonatic fraction, but also, a fixed value (of nearly a 25 wt %), is found for plagioclase minerals within the siliciclastic part.

Furthermore, when considering both the carbonate and the plagioclase distribution patterns in the entire Bay (figures 5a and 6c), a cross-linked behaviour can be observed which follows the gradient directions. This situation is clearly shown in figures 7a and 7b, where the profiles representative of the plagioclase (wt %) vs calcium carbonate (wt %) contents were plotted through length- and cross-sections of Bayona Bay (LL' and CC' in figure 1). These trends are specific for the plagioclase and do not apply to other terrigenous minerals, such as the K-feldspar microcline, although, despite their similar mechanical and chemical properties, a similar response to the dynamic regime should be expected (figure 7c).

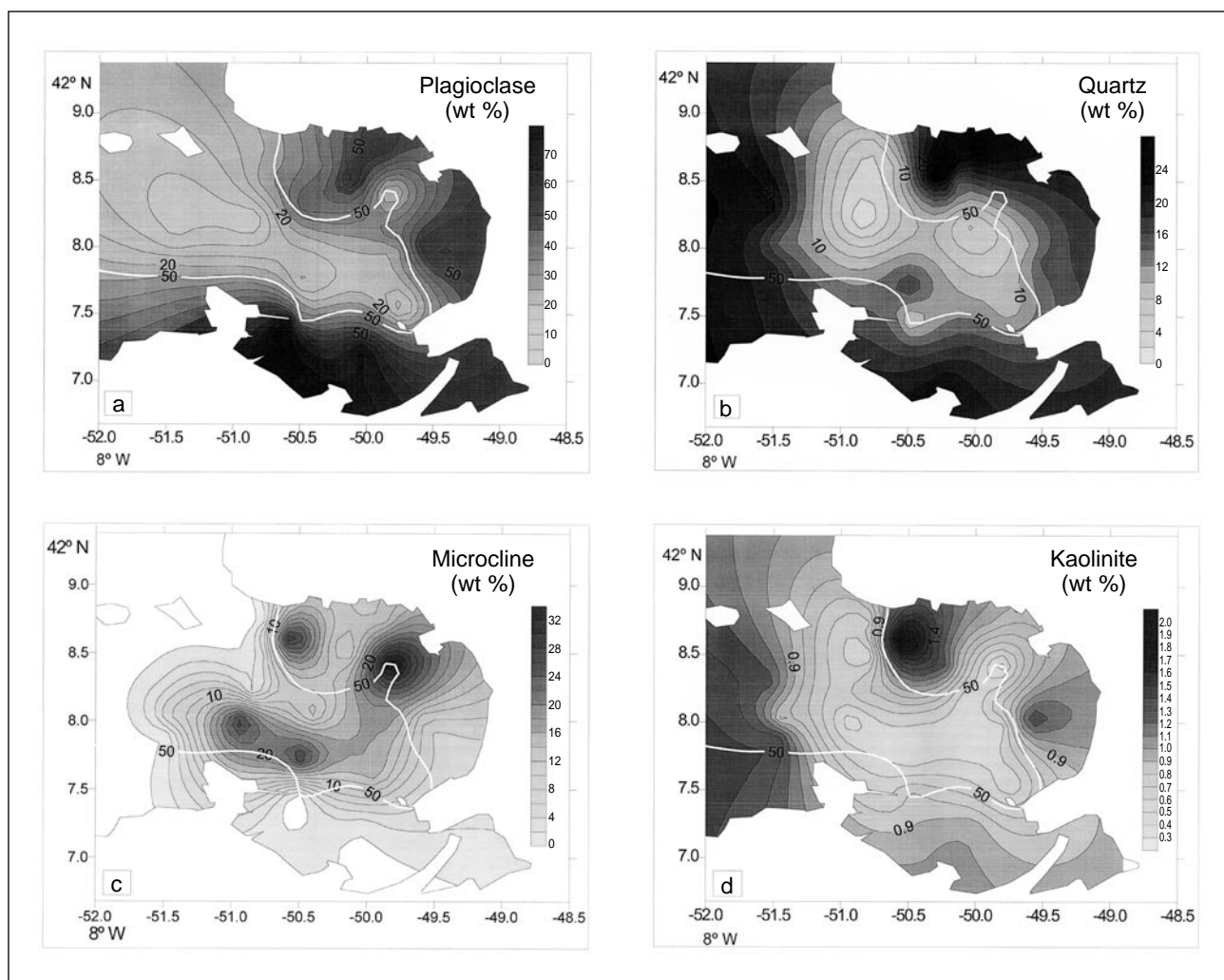
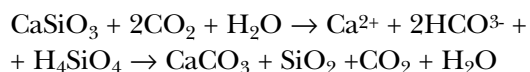


Figure 5. Single-mineral patterns for the main minerals involved in the siliciclastic fraction

The above features suggest that a sink-source mechanism operates between the primary Ca-deliverer from the terrigenous fraction (i.e. plagioclases, with an average composition between Oligoclase-Bytownite in the area) and the carbonate amount mediated by the rate of dissolved CO_2 consumption.

This equilibrium agrees with the well-known Urey expression, given the general balance equation between silicate weathering and calcium carbonate formation (France-Lanord and Perry, 1997). Schematically, it can be expressed as



where for every mol of Ca^{2+} delivered by chemical weathering of plagioclases, a mol of CO_2 is released

from the seawater to form (i.e. by *in situ* biomineralisation) a mol of calcium carbonate. It must be pointed out that CaSiO_3 in the previous equation is interpreted, in a wider perspective, as representing any calcium silicate, not simply wollastonite (Berner, 1971; Krauskopf and Bird, 1995; Berner, Lasaga and Garrels, 1983).

Obviously, the presence of a spatial pattern of mixing reflecting a stationary distribution determined by chemical constraints can be offset by the rate of material removal during highly dynamic events which apparently work in an opposite way.

Nevertheless it must be pointed out that the dissolution rate of the siliciclastic mineral to reach a steady state of dissolved cations in seawater lies on the order of a few days, which is quite fast, when compared to the periodicity of highly dynamic events. Furthermore, when dissolution and growth

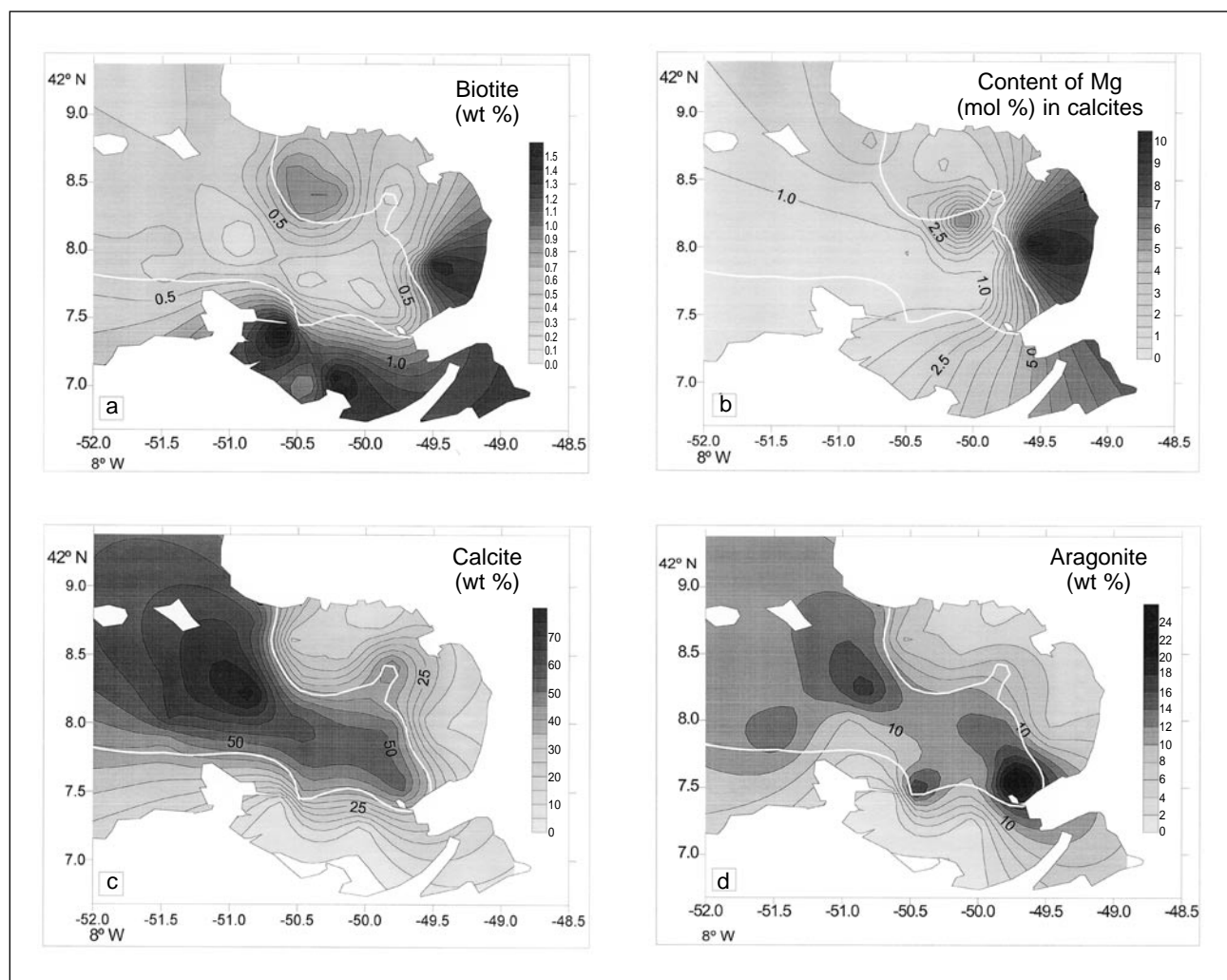


Figure 6. Specific patterns for the calcium carbonate polymorphs, Mg-distribution in calcites and biotite (see text)

processes between minerals are mutually implied, the existence of a high rate of material removal will tend to amplify these processes and produce not only two opposite abundance patterns, but also a coupled granulometric distribution. This process can be analysed as follows:

Let us consider a local site, at the seawater-sediment interface, where the plagioclase minerals are dissolving and, in turn, induce *in situ* carbonate growth (i.e. through biomineralisation). As the dissolution is a surface-controlled process, the smaller plagioclase crystals will tend to dissolve faster; consequently, when the total amount of plagioclases at the site decreases, their average grain-size increases progressively. This mechanism proceeds parallel to the increase in carbonate grain-size during growth. Therefore, during the time-evolution of the site, the same directions apply for the grain-sizes of both

minerals, coupled with an inverse trend in their relative amounts.

To obtain general patterns exhibiting such characteristics, a high rate of material removal will be needed. In such a case, following a highly dynamic event, a new non-equilibrium situation, for the total amount of both phases, will occur, and a new grain-dependent dissolution process will be reinitiated.

As a result, the long-term evolution of this process for the entire environment will be reflected in general averaged patterns for the materials involved in the dissolution and growth. These are characterised by a cross-linked distribution in the amount of materials (in wt %) and a direct relation to the number of particles for every phase associated with a particular grain size.

Consequently, a chemically constrained steady state linked to Ca behaviour can explain the nearly

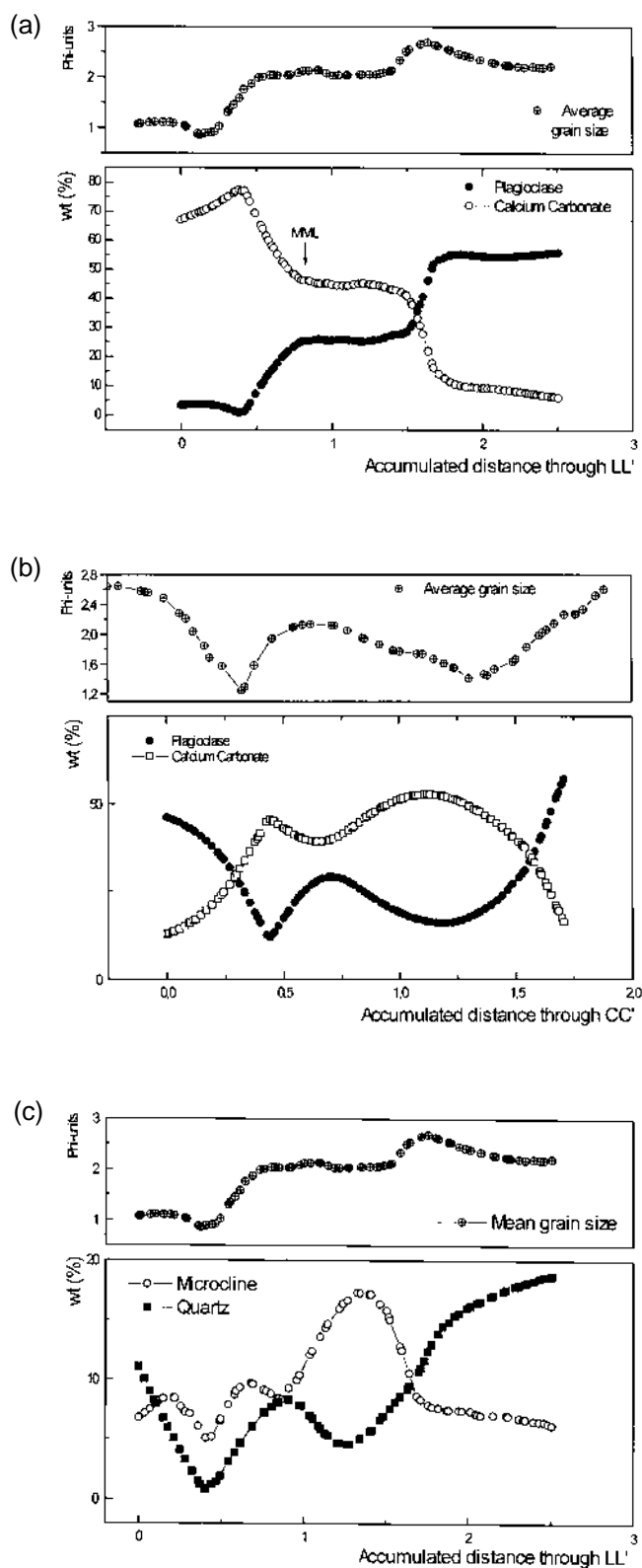


Figure 7. (a,b): Profile lines for the relative plagioclase-calcium carbonate amounts (wt %) through their length and cross-sections of Bayona Bay. (LL', CC' in figure 1). The corresponding mean grain sizes, from the settling tube analysis are also shown. (c): Variation of Q and microcline along LL'

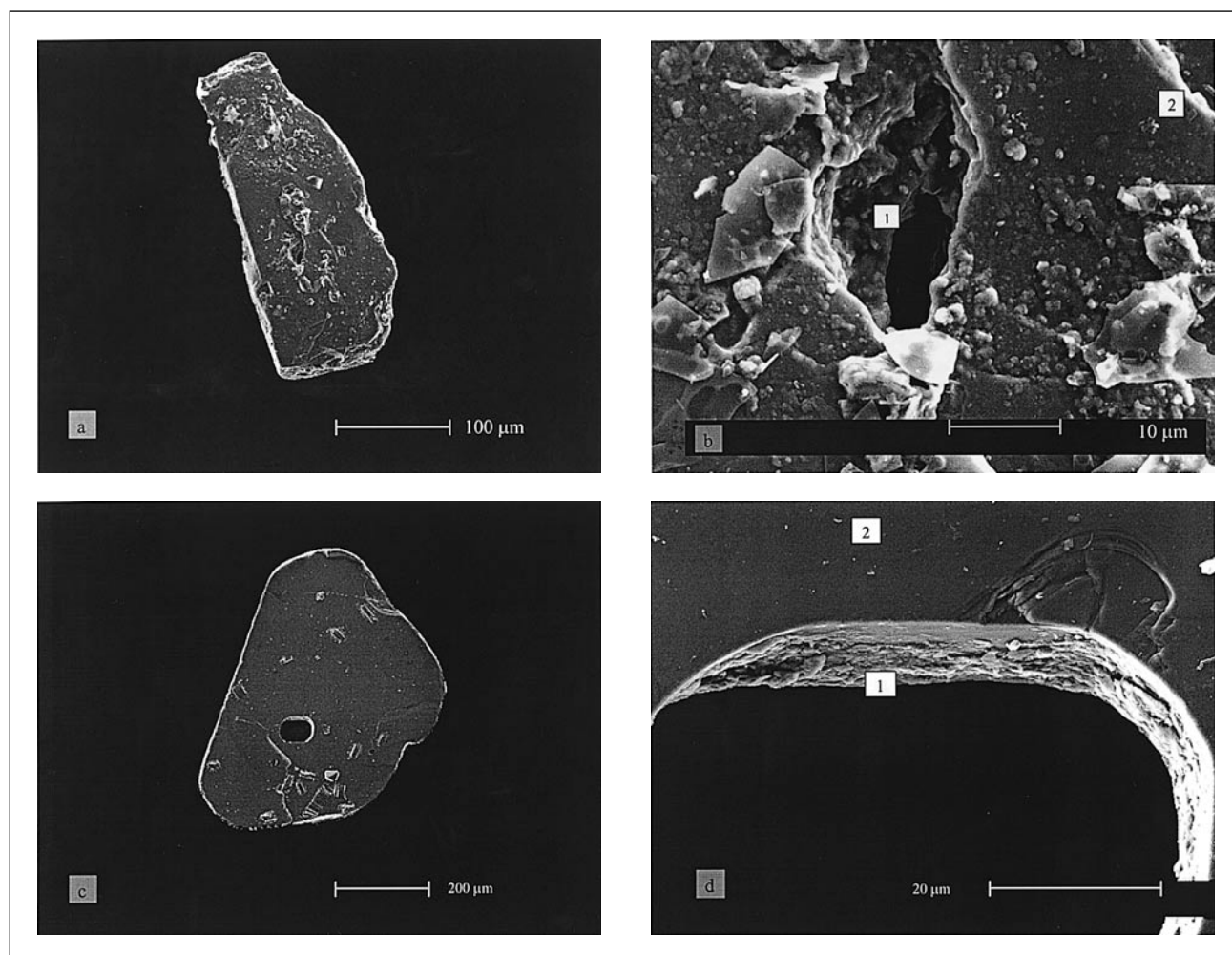


Figure 8. SEM micrographs showing dissolution processes in Ca plagioclases (a,b) and K-feldspar (c,d). Labels (1) and (2) correspond to the internal and surface regions where the EDX analysis were performed

exact opposite behaviour observed in the mineralogical patterns of the plagioclase and carbonate fractions.

In addition, a rather different behaviour was observed for the mineral patterns of the remaining terrigenous minerals not involved in the calcium carbonate generation (figures 5b, 5c, 5d). These minerals follow markedly anisotropic patterns, which are linked to lithological differences at the source areas, grain-size selection, or chemical relations between primary-secondary mineral formation within the siliciclastic fraction itself.

Evidences of dissolution processes in feldspars are shown in the SEM for Ca-plagioclase (figure 8a,b) and K-feldspar (figure 8c,d). In both cases, the EDX analysis shows a marked compositional difference between the internal region (1) and the mineral surface (2). In the case of plagioclase, the

amount of Ca decreases from a value of 16 wt % to 1 wt % at the surface. The K-content in K-feldspar also decreases from 15 wt % to 7 wt %. This suggests that an incongruent dissolution mechanism can take place, by dissolving Ca and K at a specific rate that depends on the processes involved in the general balance for the cation in the seawater and the rate of secondary mineral formation.

The latter situation was found to occur for the secondary mineral kaolinite. In this case, an intermediate trend is observed, which suggests a coupled chemical-dynamical behaviour mediated by the K-feldspar weathering. In fact the space-distribution of microcline, as primary K-supplier in this region, shown 3 maximum concentration values (M1, M2, M3) in figure 9. They can act as reservoirs for kaolinite formation. When compared with the actual maxima (K1, K2, K3) in kaolinite, no

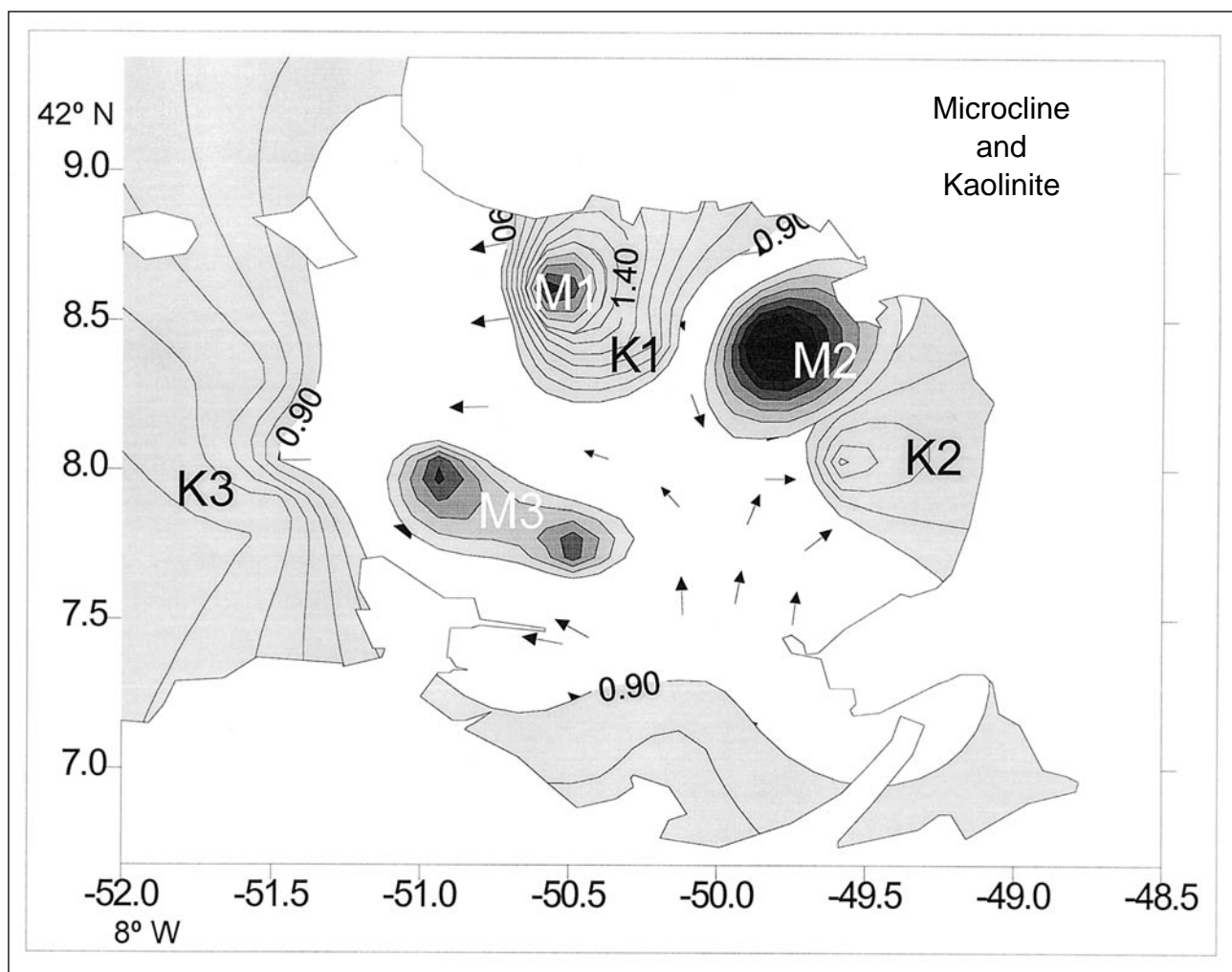


Figure 9. Source-sink model between K-feldspar weathering and secondary kaolinite generation (see text)

straightforward correlation is found. Nevertheless, the addition of the flux lines showing the main removal directions (indicated by arrows in figure 9), gives a picture that explains the main features in the actual kaolinite distribution from the main K-feldspar reservoirs.

Selective calcite-aragonite-HMG mixing in the low material removal areas

A detailed analysis of the terrigenous to carbonatic interactions can be performed when we consider the single patterns leading the space distribution for every calcium carbonate modification (calcite and aragonite).

In this case, several features can be observed by comparing figures 6c and 6d. First, there is a non-

homogeneous distribution of maxima across the MML, relative to aragonite and different to the trends followed by calcite. This is obviously a mechanical selection, given that accumulation in accordance with the crystal structure criteria is unlikely (especially when, as is the case, we move across a line with constant average grain size).

Furthermore, comparison with the biotite distribution through this MML (figure 6a) shows the following cross-correlation between the biotite maxima and the calcite, HMC, and aragonite distributions:

Zone 1. The maximum concentration of biotite coincides with the minimum of calcite and increases the aragonite contents.

Zone 2. Intermediate values of biotite favour the formation of magnesian calcite.

This compositional variation can be more clearly seen in figure 10. In this case, profiles relating

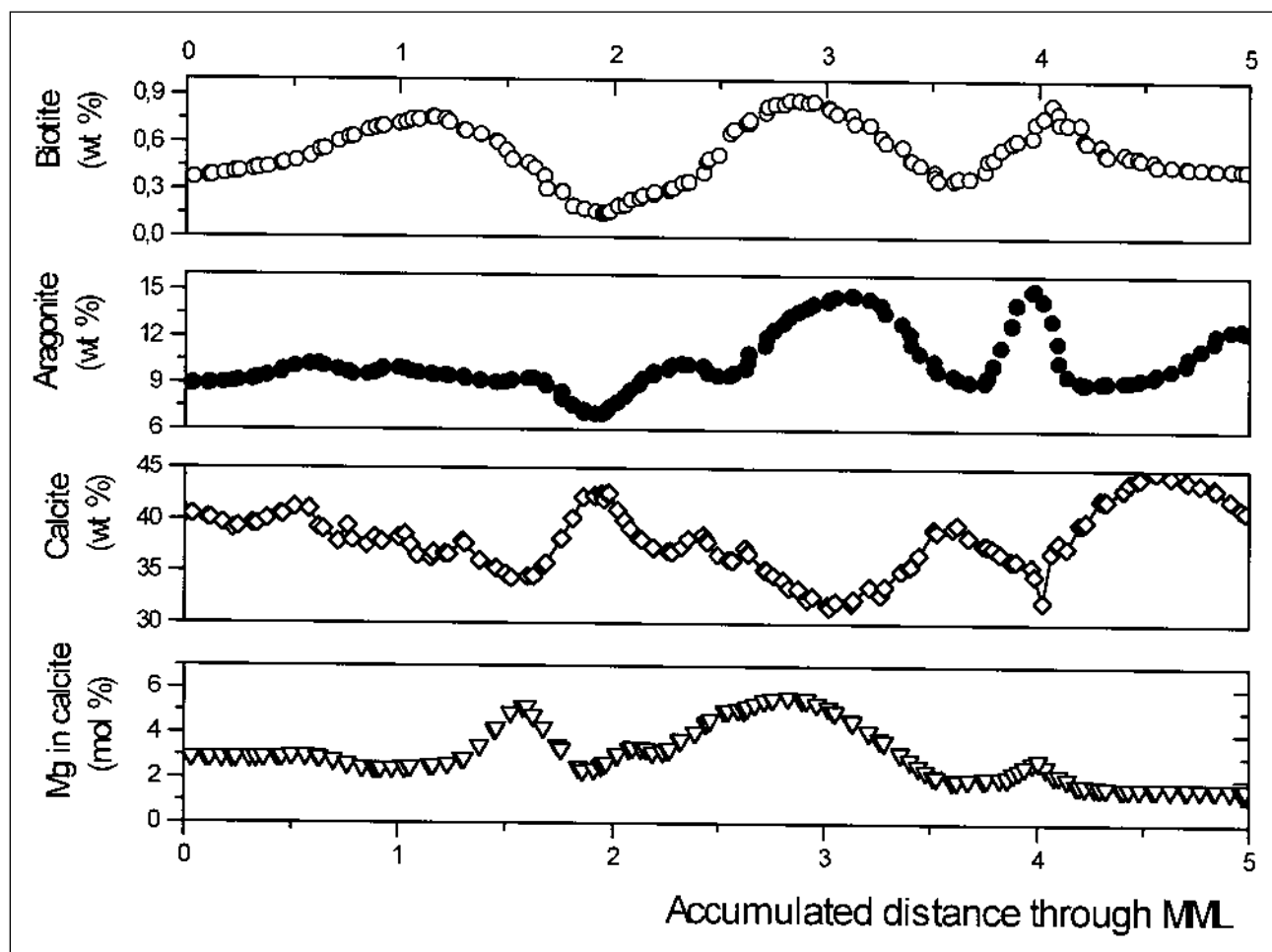


Figure 10. Profile lines showing the interactive behaviour between biotite, aragonite, calcite and HMC through the MML (see text)

the biotite, calcite and aragonite contents vs the accumulated distance across the MML are represented. As can be seen, the calcite concentration behaves opposite to those of aragonite and biotite. In addition, the Mg content of calcites increases as the total amount of calcite decreases, in good agreement with the higher solubility of the Mg calcites.

It is well known that biotite is the primary supplier of Mg to seawater through chemical weathering, which, in turn, plays an important role in processes such as the nucleation of calcium carbonate.

Magnesium ions have a marked inhibitory effect on the precipitation of calcite from seawater, but not on aragonite (Tucker and Wright, 1990). The reason is that Mg^{2+} ions fit more easily into the calcite lattice, but since Mg^{2+} ions are smaller than Ca^{2+} , they have a higher surface charge attracting a larger hydration sphere (Reeder; 1983, Fernández-

Díaz *et al.*, 1996). Consequently the solubility of calcite increases with increasing Mg^{2+} content – calcite with 0.12 moles MgCO_3 has a similar solubility to aragonite in distilled water (Walter, 1983)– but does not vary the solubility of aragonite (figure 11).

It must be pointed out that the true driving force for selective precipitation of aragonite is the $\text{Mg}^{2+}/\text{Ca}^{2+}$ ratio, instead of the absolute Mg^{2+} value. In the case of the line under study, the Ca^{2+} distribution at the mineral-seawater interface can be related to the plagioclase content as the primary Ca^{2+} supplier and provides a constant value for this mineral (and hence the Ca^{2+} content). Then an effective increase on the $\text{Mg}^{2+}/\text{Ca}^{2+}$ ratio can be expected, following the biotite distribution through this line.

The dissolution rate of stoichiometric biotite, in laboratory (Turner *et al.*, 1995), lies on the order of $10^{-16} \text{ mol Mg m}^{-2} \text{ s}^{-1}$, and is expected to release 0.16

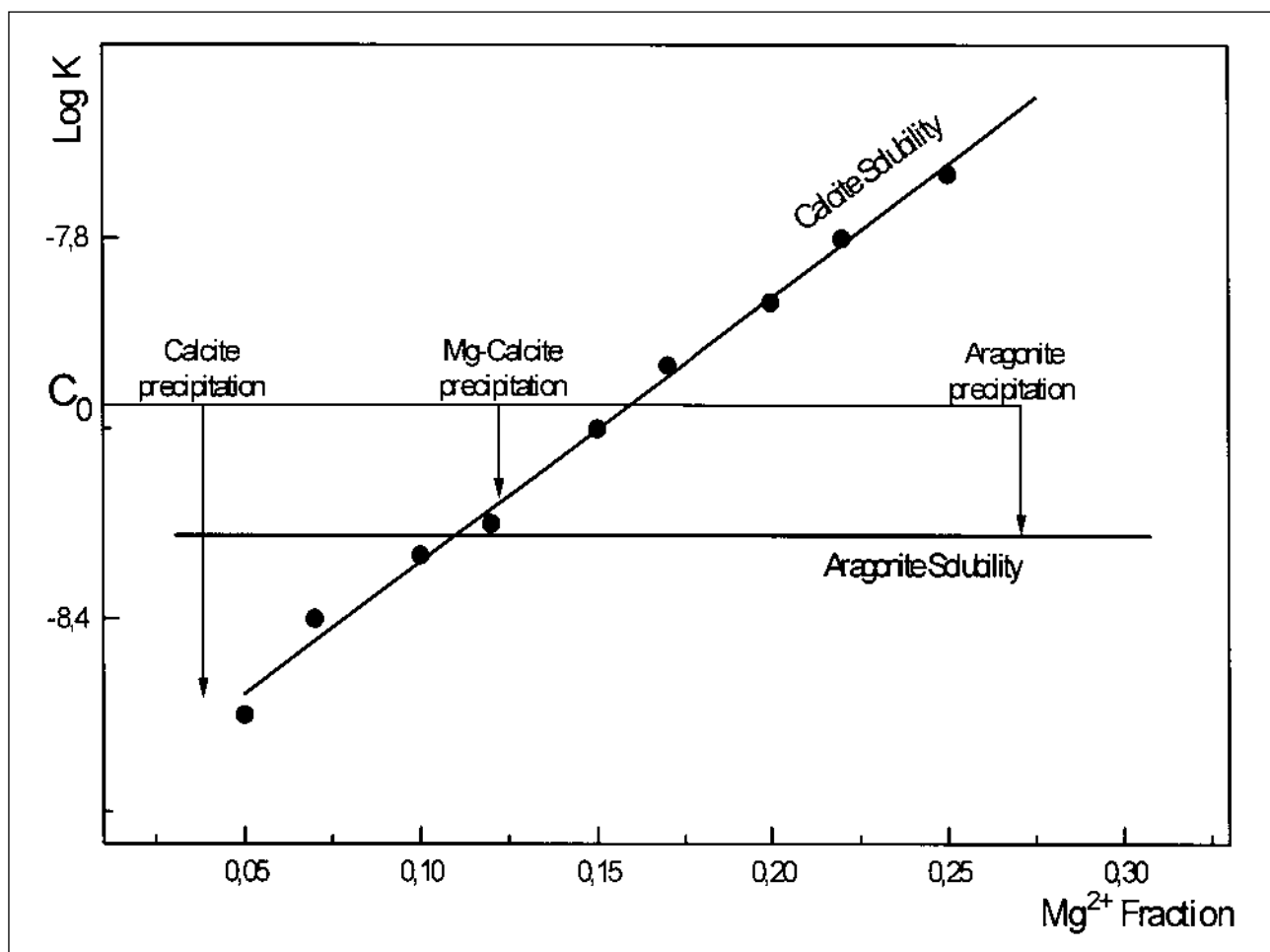


Figure 11. Several possibilities of selective polymorphic precipitation in calcium carbonate as a function of the calcite solubility vs. Mg^{2+} (mol-in calcite). Aragonite solubility, independent of the Mg content, is also shown

mols of Mg per mol of bicarbonate. These values are significant, according to the solubility diagram from Morse and Mackenzie (1990) (figure 11), to promote aragonite precipitation. Furthermore, also according to experimental studies (Malmström and Banwart, 1997) the time-lag to attain a stationary Mg^{2+} concentration value after removal from solutions is very short (on the order of 10 days).

This fact is relevant in order to explain why, even in environments with frequent highly dynamic events (i.e. storms, in the area under study) a chemical signature remains that reflects nearly perfectly steady-state calcite-to-aragonite amounts and a Mg^{2+}/Ca^{2+} ratio induced by a particular configuration of the terrigenous sediments involved in Ca-Mg supply.

It is obvious that a far-from-equilibrium configuration will transitionally take place after an event involving high energy, the amount of removed material being a measure of the distance to the steady-state

configuration. Nevertheless, the short period needed to attain a new stationary value for the dissolved amount of Ca and Mg suggests that the return to the steady-state, at a particular site on the seawater-sediment interface, is faster than the removal processes and rate-controlled by either the kinetics of selective carbonate dissolution or by carbonate growth. In the latter case, it can be expected that the choice of the specific polymorph, better adapted to the equilibrium conditions for a particular site, will result from the faunistic control over the *in situ* carbonate generation through biomineralisation.

CONCLUSIONS

The above analysis based on the comparison between the averaged distribution pattern and single-mineral distribution patterns suggests that the sig-

nature of chemical constraints, mainly connected to dissolution and growth processes, is present in the steady-state distribution of mixed silicilastic-carbonated environments.

The distribution of the carbonate components from the single mineral mapping reflects not only a grain-size dispersion in accordance with the energy, but also a general behaviour that suggests the chemical control of the Ca-suppliers from the terrigenous fraction. Furthermore, the presence of spatial non-homogeneities associated with the different calcium carbonate polymorphs, calcite and aragonite, as well as for the HMC, have been analysed following lines of constant content for plagioclase as the primary Ca supplier and with an average grain size. The observed distribution suggests that specific amounts of aragonite/calcite/HMC can be correlated with the biotite-rich zones inducing local variation in the Mg^{2+}/Ca^{2+} ratio.

ACKNOWLEDGEMENTS

The authors like to thank C. Serra and J. Millos from the University of Vigo research centre (CACYT) for their technical support in the experimental work (SEM and XRD). The present paper is a contribution to the Comisión Interministerial de Ciencia y Tecnologías (CICYT) project MAR 95-1953.

REFERENCES

- Alejo, I. 1994. *Estudio Dinámico y Sedimentario de la Bahía de Bayona*. Doctoral thesis. Universidad de Vigo. Spain: 263 pp.
- Berner, R. A. 1971. *Principles of Chemical Sedimentology*. McGraw-Hill. New York: 240 pp.
- Berner, R. A., A. C. Lasaga and R. M. Garrels. 1983. The carbonate-silicate geochemical cycle and its effect on atmospheric carbon dioxide over the past 100 m.a. *American Journal of Science* 283: 641-683.
- Bischoff, W. D., F. C. Bishop and F. T. McKenzie. 1983. Biogenically produced magnesian calcite: inhomogeneities in chemical and physical properties, comparison with synthetic phases. *American Mineralogist* 66: 770-776.
- Bish, D. L. and J. E. Post. 1993. Quantitative mineralogical analysis using the Rietveld full-pattern fitting method. *American Mineralogist* 78: 932-940.
- Fernández-Díaz, L., A. Putnis, M. Prieto and C. V. Putnis. 1996. The role of magnesium in the crystallization of calcite and aragonite in a porous medium. *Journal of Sedimentary Research* 66: 482-491.
- France-Lanord, C. and L. A. Perry. 1997. Organic carbon burial forcing of the carbon cycle from Himalayan erosion. *Nature* 390 (6): 65-67.
- Goldsmith J. R., D. L. Graf and H. O. Heard. 1961. Lattice constants of calcium-magnesium carbonates. *American Mineralogist* 46: 453-457.
- Hill, R. J. 1993. Data collection strategies: fitting the experiment to the need. In: *The Method Rietveld*. R. A. Young (ed.). Oxford Science Publications. Oxford.
- Klug, H. P. and L. E. Alexander. 1974. *X-ray Diffraction Procedures for Polycrystalline and Amorphous Materials*. Wiley-Interscience. New York.
- Krauskopf, K. B. and D. K. Bird. 1995. *Introduction to Geochemistry*. McGraw-Hill. New York. 647 pp.
- Malmström, M. and S. Banwart. 1997. Biotite dissolution at 25 °C: The pH dependence of dissolution rate and stoichiometry. *Geochimica et Cosmochimica Acta* 61: 2779-2799.
- Morse, J. W. and F. T. Mackenzie. 1990. *Geochemistry of Sedimentary Carbonates*. *Developments in Sedimentology* 48: 707 pp. Elsevier. Amsterdam.
- Mount, F. 1984. Mixing of siliclastic and carbonate sediments in shallow shelf environments. *Geology* 12: 432-435.
- Mumme, W. G., G. Tsambouraki, I. C. Madsen and R. J. Hill. 1996. Improved petrological modal analyses from X-ray powder diffraction data by use of the Rietveld method. Part II: Select sedimentary rocks. *Journal of Sedimentary Research* 66: 132-138.
- Post, J. E. and D. L. Bish. 1989. Rietveld refinement of crystal structures using powder X-ray diffraction data. Modern powder diffraction. *Reviews in Mineralogy* 20: 277-308.
- Reeder, R. J. 1983. Carbonates: Mineralogy and Chemistry. *Reviews in Mineralogy* 11: 393 pp. Washington.
- Rietveld, H. M. 1967. Line profiles of neutron powder-diffraction peaks por structure refinement. *Acta Crystallographica* 22: 151-152.
- Rietveld, H. M. 1969. A profile refinement method for nuclear and magnetic structures: *Journal of Applied Crystallography* 2: 65-71.
- Rodríguez, J., M. Anne and J. Pannetier. 1987. A system for time-resolved data analysis (Powder Diffraction Pattern). IIL Internal Report 87R014T. Institut Max Von Laue Paul Langevin. Grenoble: 127 pp.
- Rubio-Navas, J. 1981. Hoja MAGNA 223 (1): 50000. Instituto Geológico y Minero de España. Madrid.
- Tucker, M. E. and V. P. Wright. 1990. *Carbonate Sedimentology*. Blackwell. London: 482 pp.
- Turner, B. F., S. F. Murphy, S. L. Brantley, A. F. White and A. E. Blum. 1995. *Chemical weathering processes in a tropical rain forest soil, Puerto Rico*. Geological Society of America Annual Meeting. Abstracts with Programs. 67 (6): A235.
- Walter, L. M. 1983. *The Dissolution Kinetics of Shallow Water Carbonate Grain Types. Effects of Mineralogy, Microstructures and Solution Chemistry*. Ph. D. Thesis. University of Miami. Miami. Florida: 318 pp.